An ESR Study on the Heterogeneity of Dynamics in a Nematic Polymer Induced by Thermal Annealing in the Isotropic Melt

Laura Andreozzi,* Massimo Faetti, Marco Giordano, and Diego Palazzuoli

Dipartimento di Fisica, Università di Pisa and UdR INFM, Via F. Buonarroti 2, I-56127 Pisa, Italy

Giancarlo Galli

Dipartimento di Chimica e Chimica Industriale, Università di Pisa, Via Risorgimento 35, I-56126 Pisa, Italy

Received February 15, 2001; Revised Manuscript Received June 13, 2001

ABSTRACT: Heterogeneities induced in a nematic polymethacrylate by thermal annealing in the isotropic phase were investigated by studying the dynamics of the cholestane spin probe dissolved in the host matrix by electron spin resonance. The molecular site distribution was well described by a two δ-like distribution function. The temperature dependences of the dynamics of the slow and fast components were fully characterized in going from the isotropic state to the glassy state through the nematic phase. It was found that the behaviors of the spinning correlation times with temperature in the isotropic and nematic regions were well represented by the Vogel−Fulcher law. By comparing the temperature dependence of the probe dynamics with the α relaxation process of the polymer, we estimated the cooperativity degrees in the dynamics of the molecular probe in the different sites. The relative populations of the slow and fast sites were determined over the whole temperature range investigated. It was shown that such population was sensitive to conformational change of the polymer backbone.

Introduction

In the few last years side group liquid-crystalline polymers (SGLCPs) have largely been investigated due to their potential application as media for optical information storage.[1,2] Specifically, SGLCPs with azobenzene side groups appear to be very promising media for optical recording on the nanometer length scale.[3−6] Bit sensitivity and homogeneity at a molecular level are two crucial factors when considering materials for this particular application. Different spatial−temporal heterogeneities may dramatically affect the stability of the imprinted, e.g., photochemically, information into the azobenzene polymer matrix, thereby seriously limiting or preventing such practical application.

Electron spin resonance (ESR) spectroscopy, due to the anisotropy of the involved magnetic tensor, has turned out to be a powerful tool to investigate molecular dynamics, especially rotational dynamics, in simple and complex liquids.[7−10] In liquids of medium or high viscosity, ESR studies have indeed proved to be very sensitive to the details of the molecular reorientation specifically in the slow-motion regime.[11−13] Its capability is based on the ESR line shape sensitivity to the correlation function of Wigner rotation matrixes of every even rank appearing in the expression of the conditional probability pertinent to the particular stochastic reorientational model.[14] Diamagnetic systems are often investigated by dissolving suitable paramagnetic tracers, so-called spin probes, in very small quantities in a host matrix.[7] Nitroxide radicals are suitable spin probes because of their chemical and thermal stabilities and the ease of synthesizing them in a large diversity of structures and geometries.[15] In the case of the nitroxide spin probe, X band ESR experiments are sensitive to rotational dynamics for microscopic time in the interval

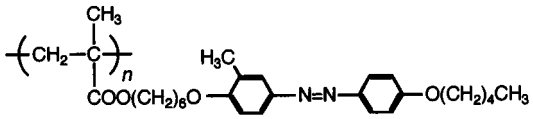

Figure 1. Formula of the repeat unit of nematic PMA.

10^{-12} s $< \tau <$ 10^{-7} s. The lower and upper limits correspond to the fast- and ultra-slow-motion regimes, respectively, in the latter region the value of correlation time being longer than the inverse of the least anisotropy of the components of the involved magnetic tensor. The cholestane spin probe has proved to be an excellent molecular tracer, especially in the study of reorientational processes of liquid-crystal polymers.[16,17]

In this work we investigated the reorientational dynamics of the cholestane molecule, which falls in the slow-motion region due to its geometry and the high viscosity of the polymeric matrix. The analysis of the ESR line shape was performed by a theoretical approach based on generalized Mori theory.[13] This allowed us to evaluate the heterogeneities and cooperativity degrees that were induced by the thermal annealing in the isotropic phase of a SGLCP with azobenzene side groups.

The SGLCP under investigation (acronym PMA) was a nematic polymethacrylate containing a 3-methyl-4′-(pentyloxy)azobenzene mesogenic unit connected at the 4-position by a hexamethylene spacer to the main chain (Figure 1). It was evidenced that thermal annealing in the *isotropic melt* could modulate different sites in the polymer which were variously populated on changing the temperature from the isotropic to the glassy state through the nematic phase.

Materials and Experimental Details

PMA was synthesized following a literature general procedure.[18] It formed a nematic phase between the glass transition temperature ($T_g = 294$ K) and the nematic−isotropic transition

* To whom correspondence should be addressed. E-mail: laura.andreozzi@df.unipi.it.

10.1021/ma010274m CCC: $20.00
Published on Web 09/11/2001

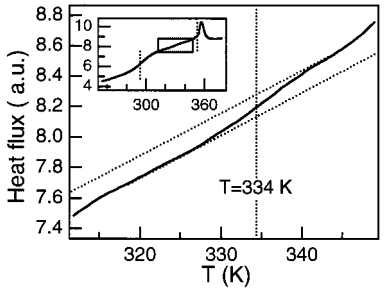

Figure 2. DSC heating trace for PMA with an enlarged region.

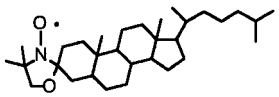

Figure 3. Structure of the cholestane spin probe.

Table 1. Physicochemical Parameters of Nematic PMA

M_w	M_w/M_n	T_g (K)	T_{NI} (K)	ΔH_{NI} (J/g)
59000	3.17	294	353	1.8

Table 2. Values of the Principal Components of the Zeeman and Hyperfine Tensors in the Molecular Reference Frame for the Cholestane Spin Probe

g			**A** (G)		
g_{xx}	g_{yy}	g_{zz}	A_{xx}	A_{yy}	A_{zz}
2.0026	2.0092	2.0069	32.6	5.5	5.0

temperature (T_{NI} = 353 K). Data of molecular weights and dispersities and transition temperatures are reported in Table 1.

Differential scanning calorimetry measurements were carried out with a Perkin-Elmer DSC7 apparatus that had been calibrated with indium and zinc standards. For the annealing experiments, the sample (ca. 15 mg) was first heated for 4 h to 383 K, which is well above T_{NI}, then rapidly cooled to 250 K, and finally heated to the isotropic melt. A typical DSC curve is shown in Figure 2, together with an enlarged particular step occurring at about 334 K.

ESR studies were performed on PMA samples in which the cholestane probe was dissolved. The structure of cholestane (Aldrich) nitroxide spin probe[19] is reported in Figure 3.

The sample was prepared at room temperature by mixing two chloroform solutions containing predetermined amounts of polymer and cholestane, respectively. The resulting solution (10^{-3} cholestane/repeat unit molar ratio) was evaporated to complete dryness by being heated to 358 K under vacuum for ca. 72 h. The sample was finally sealed in a standard ESR tube. The sample was annealed in the isotropic phase at T_a = 383 K for 4 h, after which a stable ESR spectrum was recorded that then showed no changes after longer annealing times. The sample was then cooled to a predetermined temperature (shown by an arrow in Figure 7), and ESR spectra were recorded over a set of decreasing temperatures in such a way that the overall period of recording time t_R was 1.5 h. After this set was completed, the sample was taken back to 383 K and annealed there for a time t_w of 2 h, which ensured attainment of equilibrium conditions before recording over the following set of decreasing temperatures was started. By this procedure, the temperature range 383−280 K was fully investigated. Spectra in the upper temperature region were simply recorded on slowly heating the sample from 383 to 420 K.

The principal components of the magnetic tensors of the spin probe were drawn by the powder line shape[20] of the linear ESR recorded at 143 K, according to the procedure detailed elsewhere.[16] The values of the Zeeman and hyperfine tensors in the molecular frame are listed in Table 2. The cholestane spin probe exhibits nearly axial symmetry. Its reorientational dynamics in a PMA matrix is characterized by a spinning motion, around its own symmetry axis, and a tumbling motion of the symmetry axis itself with correlation times $\tau_{||}$ and $\tau_{\perp}$, respectively. The anisotropy ratio between them was found to be $\tau_{\perp}/\tau_{||}$ = 15 over the whole temperature range. Due to this relationship, in this work only the temperature dependence of $\tau_{||}$ will be shown.[21]

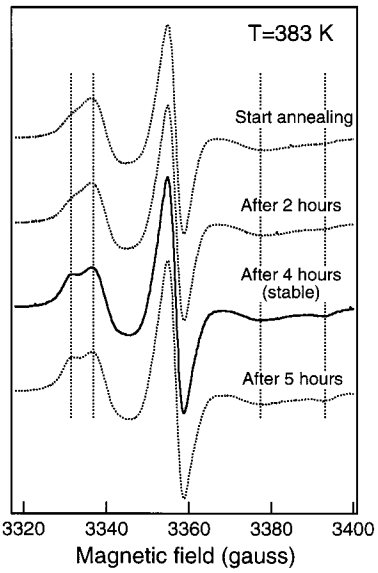

Figure 4. Time evolution of the ESR line shape during annealing at T_a = 383 K.

ESR measurements were performed by an X band Bruker ER 200 SRL, and the control of temperature was assured by a Bruker BVT100 system with ±0.1 deg accuracy.

Results and Discussion

It is well-known that the ESR line shape is sensitive to local environments that modulate the diffusional process of molecular tracers in simple fluids.[7] ESR studies have also shown their capability to probe local order and dynamics in polymers,[17,22−25] even though an accurate evaluation of the reorientational processes of the paramagnetic molecules in highly heterogeneous systems has very seldom been performed.[26,27] Moreover, memory effects due to thermal history substantially complicate the analysis. Therefore, special care was devoted in this work to singling out the suitable experimental conditions for achieving reproducible responses of the polymer sample during the measuring time with the aim to identify memory effects on the polymer structural relaxation and, therefore, on the relaxation on the time scale of the probe (see the Materials and Experimental Details).

The temperature dependence of the reorientational correlation times and the evolution of the redistribution of molecular tracers in the polymer sites for a selected thermal treatment were obtained.

The evolution of the experimental spectra as obtained at the annealing temperature T_a = 383 K until a stable spectrum was eventually reached (4 h) is illustrated in Figure 4. The vertical dotted lines point out the spectral features signaling two different sites for the probe, namely, slow (outer) and fast (inner) components. A comparison between the stable ESR spectrum with the one after 2 h of annealing clearly shows the increasing contribution from the slow component of the ESR line shape with annealing time up to a saturation value (see below).

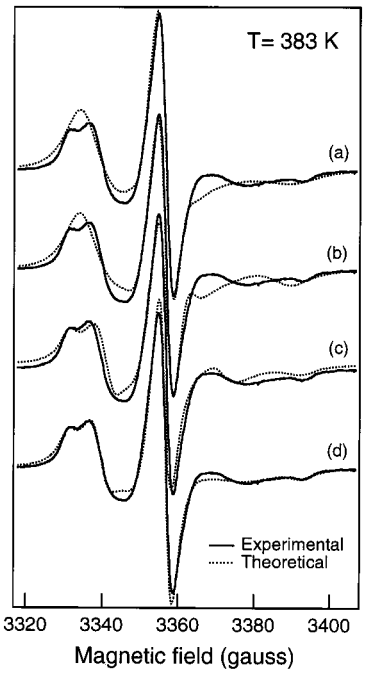

Figure 5. Comparisons between ESR experimental and theoretical spectra ($T_a = 383$ K) with different reorientational models and distribution functions: (a) diffusional; (b) anisotropic jump; (c) diffusional and log-Gauss distribution; (d) diffusional and two δ distribution functions.

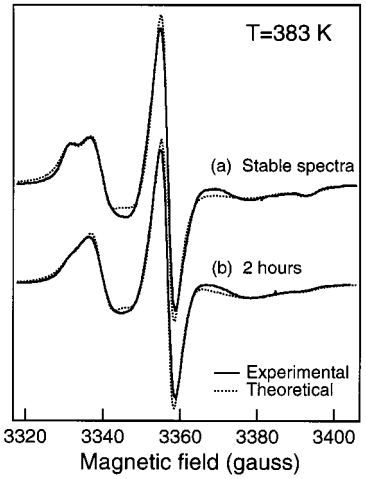

Figure 6. (a) ESR stable spectrum and best fit. (b) ESR spectrum after 2 h of annealing and best fit.

Careful simulations were carried out to confirm the bimodal character of the distribution function of the spin probe sites (Figure 5). A two δ-like distribution function was shown to provide a better simulation than log-Gauss and square distributions. A bimodal log-Gauss distribution did not improve the goodness of the fit. The detailed study of the efforts to get better representation is reported elsewhere.[26]

Parts and b of Figure 6 illustrate the fairly good simulation of both the stable spectrum and the one for the sample annealed for 2 h, respectively.

Table 3 summarizes data relative to the theoretical spectra compared in Figure 6 with the experimental ones.

One notes the growth of the slow component at the expense of the fast component after 4 h of annealing. However, the determined values of the spinning correlation times were the same within experimental error.

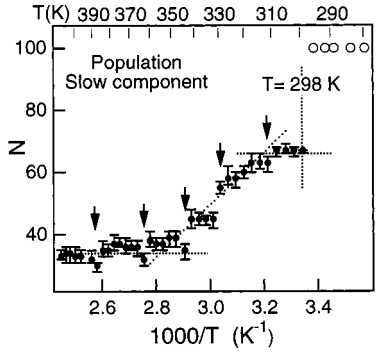

Figure 7. Slow spin population normalized to 100 as a function of 1000/T (the arrows point to the initial temperature of each predetermined set of temperatures after annealing at 383 K; see the text). Open circles refer to motionless components.

Table 3. Populations and Reorientational Correlation Times of Theoretical Simulation Spectra during Annealing at 383 K

spectra	$\tau_{\|\|}^s$ (s)	% slow	$\tau_{\|\|}^f$ (s)	% fast
at the start	$(1.6 \pm 0.2) \times 10^{-8}$	16 ± 4	$(1.7 \pm 0.2) \times 10^{-9}$	84 ± 5
after 2 h	$(1.8 \pm 0.1) \times 10^{-8}$	18 ± 3	$(1.7 \pm 0.1) \times 10^{-9}$	82 ± 2
after 4 h (stable)	$(1.9 \pm 0.1) \times 10^{-8}$	37 ± 2	$(1.9 \pm 0.1) \times 10^{-9}$	63 ± 2

Therefore, the annealing procedure at $T_a = 383$ K appears to only affect the relative populations of slow and fast sites present in the polymer matrix. The evaluation of the relative population of the paramagnetic probe in the slow sites over the measuring temperature range is reported in Figure 7.

At temperatures lower than the glass temperature, $T_g = 294$ K, the slow and fast components are both nearly completely motionless and can no longer be distinguished.

Three dynamic regions can be identified: (1) a high-temperature region, extending between approximately 420 and 345 K, in which the value of the slow component percentage is centered at about 37%, (2) a low-temperature region, going from about 320 K to T_g, in which the percentage population is nearly 66%, and (3) an intermediate region, whose center value is 334 K, in which the slow sites become more significantly populated on decreasing the temperature.

We suggest the relative instability of the fast component in the intermediate temperature region is due to a different conformation adopted in the host matrix by the polymer main chain as driven by the nematic ordering potential. This is consistent with the substantial change in heat capacity which was detected by DSC at the same temperature (see Figure 2). Independent investigations of the fast reorientational dynamics on the same PMA sample by LODESR spectroscopy have also shown that a conformational variation in the polymer backbone of the polymer matrix occurred at about the same temperature of 330 K.[28]

Figure 8 shows the dependence of the spinning correlation time $\tau_{\|}^f$ of the fast component of the molecular probe on temperature. Three dynamic regions can be identified as low-, intermediate-, and high-temperature regions. The crossover temperatures between the different dynamic regions almost coincided with the T_{NI} and T_g of the polymer matrix. In both high- and intermediate-temperature regions, the behavior with temperature of the $\tau_{\|}^f$ of the cholestane probe in the fast

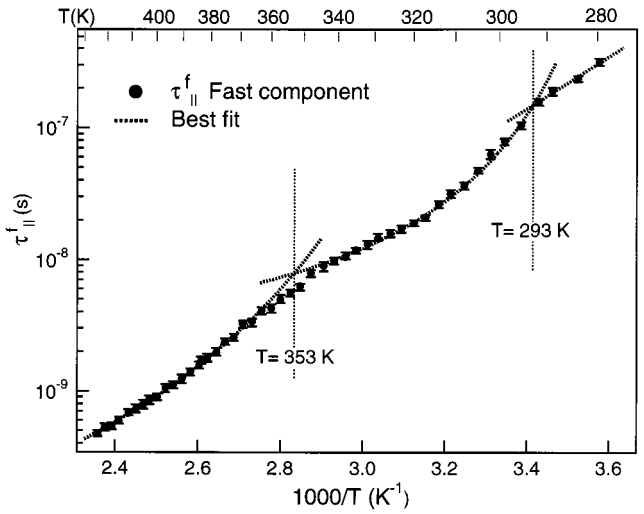

Figure 8. Fast-component correlation times $\tau_{||}^{f}$ vs 1000/T.

Table 4. Fit Parameters of the Vogel−Fulcher Law for Fast-Component $\tau_{||}^{f}$

$\tau_{||0}{}^{f}$ (s)	T_0 (K)	T_b (K)	ξ^f
High Temperature			
$(1.2 \pm 0.1) \times 10^{-11}$	259 ± 3	608 ± 27	$\xi_I^f = 0.47$
Intermediate Temperature			
$(1.4 \pm 0.1) \times 10^{-9}$	258 ± 8	164 ± 9	$\xi_N^f = 0.12$

sites could fairly well be reproduced by assuming a Vogel−Fulcher (VF) law:

$$\tau_{||}^{f} = \tau_{||0}{}^{f} \exp\left(\frac{T_b}{T - T_0}\right) \quad (1)$$

where $\tau_{||0}^{f}$ and T_b, the activation pseudoenergy (K), are constants depending also on the spin probe and T_0 is the Vogel temperature. The values of the fit parameters are reported in Table 4.

It should be noted that rheological measurements on a PMA sample subjected to the same thermal history provided a temperature dependence of the structural relaxation time in the temperature region down to 300 K that was well described by a VF law with parameters $T_0 = 259 \pm 5$ K and $T_b = 1300 \pm 50$ K.[29] Therefore, in both high and intermediate regions the spinning correlation time behavior can be expressed by a fractionary law of the structural relaxation time τ_α:

$$\tau_{||}^{f} \propto \tau_\alpha(T)^{\xi} \quad (2)$$

where ξ, the fractional exponent, may vary between 0 and 1, with $\xi = 1$ corresponding to a complete coupling of the probe dynamics to the structural relaxation of the host matrix. ξ resorts to be the ratio of the activation pseudoenergy of the VF law relevant to the dynamics of the fast component over the value of the activaction pseudoenergy of the structural relaxation time τ_α.

Many reports on fractional diffusion laws have appeared in the literature.[9,30] Fractionary behavior has been recognized by linear and nonlinear ESR studies in molecular glass formers[9,31] and in polymers.[32] A similar behavior was shown by nonradiative decay time measurements[33] in different glass formers and by fluorescence measurements in polymers.[29]

Starting from Vrentas−Duda theory[34] for the translational diffusion, an extension to rotational diffusion[31] has been proposed in which the fractionary coefficient ξ is defined as the ratio between the volume of the probe and the volume of the polymer jumping units or cooperative volume. Furthermore, a simple theoretical approach[9] based on rotational diffusion and taking into account the presence of dynamical heterogeneities led to the finding that $1/\xi$ would represent the number of cooperative molecules of the host matrix.

Linear ESR[9] studies performed on different spin probes dissolved in *molecular glass formers* have shown that the reorientational correlation times of a paramagnetic probe follow fractional laws $(\eta/T)^{\xi}$, η being the viscosity of the material of interest, over temperature ranges across the critical temperature T_c stemming from mode coupling theory.[35] On the other hand, the probe dynamics followed a Debye law at higher temperatures than the critical region around T_c. Several examples of cooperativity have been observed by ESR spectroscopies in the dynamics of the paramagnetic tracers dissolved *in polymeric materials* in temperature ranges across T_g. To our knowledge the occurrence of complete coupling between the spin probe reorientational dynamics and rheological relaxation processes in the polymeric matrix, over a large range of high temperatures, has been demonstrated in ref 36 only.

In light of the above considerations we could expect a complete coupling between tracer dynamics and the α rheological process, in the higher temperature region, that is, the isotropic state. Thus, the observed decoupling could be ascribed not to a cooperativity effect in dynamics, but rather to a steric hindrance due to the specific local characteristic of the host matrix. The expected cooperativity effect in the nematic region might be accounted for simply by defining ξ_C^f equal to ξ_N^f/ξ_I^f, where ξ_I^f and ξ_N^f are the fractionary coefficients in eq 2 relevant to isotropic and nematic regions, respectively.

In the high-temperature (isotropic) region, the decoupling degree between cholestane spin probe dynamics and PMA structural relaxation time turned out to be $\xi_I^f = 0.47$ (Table 4). The relatively high value of ξ_I^f, together with the clear sensitivity of the probe dynamics to the nematic−isotropic transition, seems to strenghten the hypothesis that the sites experienced by the probe were located in the mesogenic side groups, in agreement with previous observations on a closely related nematic polyacrylate.[17]

In the intermediate (nematic) region, the Vogel temperature coincided with that obtained in the higher temperature region, signaling that the rotational relaxation was still driven by the dynamics of the polymer main chain. It can be noted however that the activation pseudoenergy T_b was lower, implying the onset of cooperativity in spin probe dynamics due to the ordering of the polymer side groups driven by the nematic potential. The fractionary coefficient in the nematic range turned out to be $\xi_N^f = 0.12$. Therefore, the cooperativity coefficient turns out to be $\xi_C^f = \xi_N^f/\xi_I^f = 0.25$. In the frame of the Vrentas−Duda theory the cooperativity volume would consist of about $N^f = 1/\xi_C^f \cong 4$ repeat units.

As the glass transition temperature of the polymer was reached, a further change in dynamics occurred. The temperature dependence was in fact reproduced by an Arrhenius behavior whose fit parameters were $\tau_{||0}^{f} = (2.7 \pm 0.8) \times 10^{-14}$ s and $\Delta E = 3.8 \pm 0.3$ kJ/mol. The activation energy value evaluated for this region is characteristic of the cholestane spin probe in both low

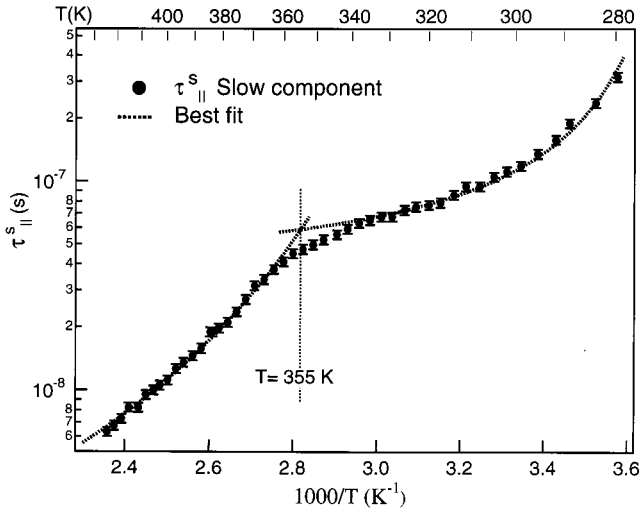

Figure 9. Slow-component correlation times $\tau_{||}^s$ vs 1000/T.

Table 5. Fit Parameters of the Vogel−Fulcher Law for Slow Component $\tau_{||}^s$

$\tau_{||_0}^s$ (s)	T_0 (K)	T_b (K)	ξ^s
High Temperature			
$(3.3 \pm 0.3) \times 10^{-10}$	259 ± 3	497 ± 4	$\xi_I^s = 0.38$
Intermediate Temperature			
$(3.6 \pm 0.3) \times 10^{-8}$	259 ± 4	47 ± 2	$\xi_N^s = 0.036$

molar mass and polymeric glasses in a nearly solidlike diffusion.

The temperature dependence of the spinning correlation time $\tau_{||}^s$ of the slow component of the paramagnetic probe is shown in Figure 9.

Analogous to the trend of the fast component, a VF equation nicely fitted the experimental data. The fit parameters are reported in Table 5.

It has to be noted that the value of the Vogel temperature was the same as that found by rheological measurements. As seen for the fast component, a strong change in dynamics occurred in correspondence with the nematic−isotropic transition, indicating that the slow sites were also located in the proximity of the mesogenic molecules. Moreover, the lower value of T_b evaluated implies a greater decoupling from the structural relaxation dynamics, despite the slower dynamics of the probe. Accordingly, the slower sites are likely situated away from the polymer main chain along the mesogenic side group near the terminal alkyl tails of the repeat unit. The coefficient ξ_I^s of the fractionary law holding at higher temperatures than T_{NI} was found to be 0.38. In the nematic temperature region the coefficient ξ_N^s turned out to be 0.036. Therefore, $\xi_C^s = \xi_N^s/\xi_I^s \cong 0.1$, which implies a definitely greater cooperative volume ($N^s \cong 10$) than that for the fast component. Finally, one should note the insensitivity of the dynamics of the slow component to T_g, which also points to the fact that the probe molecules are embedded in a soft environment. This is also consistent with the conclusion that slow sites would be situated in proximity of the alkyl tails of the repeat unit.

Conclusions

A careful simulation strategy of the ESR line shape combined with a suitable thermal annealing procedure has shown evidence of the presence of different molecular sites in the nematic PMA matrix. Their relative stabilities and populations have been established over a large temperature range. The decoupling degrees from the structural relaxation dynamics and the cooperativity volumes have been evaluated for both slow and fast sites. The emerging picture is that of a greatly heterogeneous system as far as site and cooperativity are concerned. These findings are at variance with the long-held belief that thermal annealing in the isotropic melt would erase memory effects in liquid-crystal polymers. In conclusion, the adopted annealing treatment of the nematic PMA at temperatures well above T_{NI} rendered the polymer matrix rich of defects on a nanometer length scale, and such annealing of the polymer would be unsuitable in envisioning its use as a substrate for optical nanorecording.

References and Notes

(1) *Side chain Liquid Crystal Polymers*; McArdle, C. B. Ed.; Blakie and Son Ltd: Glasgow, Scotland, 1989.
(2) Yamane, H.; Kikuchi, H.; Kajiyama, T. *Polymer* **1999**, *40*, 4777.
(3) Anderle, K.; Birenheide, R.; Werner, M. J. A.; Wendorff, J. H. *Liq. Cryst.* **1991**, *9*, 691.
(4) Eich, M.; Wendorff, J. H. *Makromol. Chem. Rapid Commun.* **1987**, *8*, 467.
(5) Bubliz, D.; Helgert, M.; Fleck, B.; Wenke, L.; Hvilsted, S.; Ramanujam, P. S. *Appl. Phys. B* **2000**, *70*, 803. Helgert, M.; Fleck, B.; Wenke, L.; Hvilsted, S.; Ramanuiam, P. S. *Appl. Phys. B* **2000**, *70*, 863.
(6) Labarthet, F. L.; Freiberg, S.; Pellerin, C.; Pezolet, M.; Natansohn, A.; Rochon, P. *Macromolecules* **2000**, *33*, 6815.
(7) *Spin Labeling*: *Theory and Application*; Berliner, L. J. Ed.; Academic Press: New York, 1976; Vol. 1; 1979; Vol. 2.
(8) *Electron Spin Relaxation in Liquids*; Muus, L. T., Atkins, P. W., Eds.; Plenum: New York, 1972.
(9) Andreozzi, L.; Di Schino, A.; Giordano, M.; Leporini, D. *Europhys. Lett.* **1997**, *38*, 669 and references therein.
(10) Imrie, C. T.; Ionesco, D.; Luckhurst, G. R. *Macromolecules* **1997**, *30*, 4597.
(11) Moro, G.; Freed, J. H. *J. Phys. Chem.* **1980**, *84*, 2837. Moro, G.; Freed, J. H. *J. Chem. Phys.* **1981**, *74*, 3757. Lee, M. H.; Kim, I. M.; Dekeyser, R. *Phys. Rev. Lett.* **1984**, *52*, 1579 and references therein.
(12) Grigolini, P. In *Memory Function Approaches to Stochastic Problems in Condensed Matter*; Evans, M. W., Grigolini, P., Pastori Parravicini, G., Eds., 1985; p 321.
(13) Giordano, M.; Grigolini, P.; Leporini, D.; Marin, P. *Phys. Rev. A* **1983**, *28*, 2474.
(14) Andreozzi, L.; Cianflone, F.; Donati, C.; Leporini, D. *J. Phys.: Condens. Matter* **1996**, *8*, 3795.
(15) Keana, J. F. *Chem. Rev.* **1978**, *78*, 37.
(16) Andreozzi, L.; Giordano, M.; Leporini, D. *Appl. Magn. Reson.* **1992**, *4*, 279.
(17) Andreozzi, L.; Giordano, M.; Leporini, D. In *Structure and Transport Properties in Organized Materials;* Chiellini, E., Giordano, M., Leporini, D., Eds.; World Scientific: Singapore, 1997; p 207.
(18) Angeloni, A. S.; Caretti, D.; Laus, M.; Chiellini, E.; Galli, G. *J. Polym. Sci, Polym. Chem. Ed.* **1991**, *29*, 1865.
(19) Carr, S. G.; Kao, S. K.; Luckhurst, G. R.; Zannoni, C. *Mol. Cryst. Liq. Cryst.* **1976**, *35*, 7.
(20) Siderer, Y.; Luz., Z. *J. Magn. Reson.* **1980**, *37*, 449.
(21) Note that an anisotropy ratio $\tau_\perp/\tau_{||} = 15$ was found over the whole temperature range for both fast and slow components (see the text).
(22) Tsay, F. D.; Hong, S. D.; Moacanin, J.; Gupta, A. *J. Polym. Sci., Polym. Phys. Ed.* **1982**, *20*, 763.
(23) Tsay, F. D.; Gupta, A. *J. Polym. Sci., Polym. Phys. Ed.* **1987**, *25*, 855.
(24) Kamaev, P. P.; Aliev, I. I.; Iordanskii, A. L.; Wasserman, A. M. *Polymer* **2001**, *42*, 515.
(25) Veksli, Z.; Andreis, M.; Rakinov, B. *Prog. Polym. Sci.* **2000**, *25*, 948.
(26) Andreozzi, L.; Faetti, M.; Giordano, M.; Palazzuoli; D. Submitted for publication.
(27) Xu, D.; Crepeau, R. H.; Ober, C. K.; Freed, J. H. *J. Phys. Chem.* **1996**, *100*, 15783 and references therein.

(28) Andreozzi, L.; Bagnoli, M.; Faetti, M.; Giordano, M. *Mol. Cryst. Liq. Cryst.*, in press.
(29) Andreozzi, L.; Faetti, M.; Giordano, M. Manuscript in preparation.
(30) Ye, J. Y.; Hattori, T.; Nakatsuka, H. *Phys. Rev. B* **1997**, *56*, 5286.
(31) Andreozzi, L.; Faetti, M.; Giordano, M.; Leporini, D. *J. Phys. Chem.* **1999**, *103*, 4097 and references therein.
(32) Andreozzi, L.; Cianflone, F.; Galli, G.; Giordano, M.; Leporini, D. *Mol. Cryst. Liq. Cryst.* **1996**, *290*, 1.
(33) Hooker, J. C.; Torkelson, J. M. *Macromolecules* **1995**, *28*, 7683.
(34) Vrentas, J. S.; Duda, J. L. *J. Polym. Sci., Polym. Phys. Ed.* **1985**, *23*, 2475; **1985**, *23*, 2489.
(35) Götze, W.; Sjögren, L. *Rep. Prog. Phys.* **1992**, *55*, 55 and references therein.
(36) Faetti, M.; Giordano, M.; Pardi, L.; Leporini, D. *Macromolecules* **1999**, *32*, 1876.

MA010274M